Journal of Orthopaedic Translation 37 (2022) 143–151

Contents lists available at ScienceDirect

Journal of Orthopaedic Translation

journal homepage: www.journals.elsevier.com/journal-of-orthopaedic-translation

Original article

In vivo prevascularization strategy enhances neovascularization of β-tricalcium phosphate scaffolds in bone regeneration

Jia Xu [a,1], Junjie Shen [a,1], YunChu Sun [a], Tianyi Wu [a], Yuxin Sun [c], Yimin Chai [a], Qinglin Kang [a], Biyu Rui [a,2,*], Gang Li [b,2,**]

[a] *Department of Orthopedic Surgery, Shanghai Sixth People's Hospital Affiliated to Shanghai Jiao Tong University School of Medicine, Shanghai, PR China*
[b] *Department of Orthopaedics and Traumatology, Li Ka Shing Institute of Health Sciences and Lui Che Woo Institute of Innovative Medicine, Faculty of Medicine, The Chinese University of Hong Kong, Prince of Wales Hospital, Shatin, Hong Kong SAR, PR China*
[c] *Department of Orthopaedics and Traumatology, Bao-An District People's Hospital, Shenzhen, PR China*

ARTICLE INFO

Keywords:
Prevascularization
Beta-tricalcium phosphate
Bone regeneration
Angiogenesis
Tissue engineering

ABSTRACT

Background: Neovascularization is critical for bone regeneration. Numerous studies have explored prevascularization preimplant strategies, ranging from calcium phosphate cement (CPC) scaffolds to co-culturing CPCs with stem cells. The aim of the present study was to evaluate an alternative *in vivo* prevascularization approach, using preimplant-prepared macroporous beta-tricalcium phosphate (β-TCP) scaffolds and subsequent transplantation in bone defect model.

Methods: The morphology of β-TCPs was characterized by scanning electron microscopy. After 3 weeks of prevascularization within a muscle pouch at the lateral size of rat tibia, we transplanted prevascularized macroporous β-TCPs in segmental tibia defects, using blank β-TCPs as a control. Extent of neovascularization was determined by angiography and immunohistochemical (IHC) evaluations. Tibia samples were collected at different time points for biomechanical, radiological, and histological analyses. RT-PCR and western blotting were used to evaluate angio- and osteo-specific markers.

Results: With macroporous β-TCPs, we documented more vascular and supporting tissue invasion in the macroporous β-TCPs with prior *in vivo* prevascularization. Radiography, biomechanical, IHC, and histological analyses revealed considerably more vascularity and bone consolidation in β-TCP scaffolds that had undergone the prevascularization step compared to the blank β-TCP scaffolds. Moreover, the prevascularization treatment remarkably upregulated mRNA and protein expression of BMP2 and vascular endothelial growth factor (VEGF) during bone regeneration.

Conclusion: This novel *in vivo* prevascularization strategy successfully accelerated vascular formation to bone regeneration. Our findings indicate that prevascularized tissue-engineered bone grafts have promising potential in clinical applications.

The translational potential of this article: This study indicates a novel in vivo prevascularization strategy for growing vasculature on β-TCP scaffolds to be used for repair of large segmental bone defects, might serve as a promising tissue-engineered bone grafts in the future.

1. Introduction

Repairing large bone defects remains a significant challenge in clinical practice. Autologous bone grafts are currently the gold standard for repair of bone defects [1,2]. However, autografting is restricted by several problems, including geometric mismatching, donor-site morbidity, and infections [3], thus limiting its utility in patients with large bone defects. These limitations have led to the emergence of bone-tissue engineering. With this technique, scaffolds are employed alone or in combination with growth factors and or stem cells to repair

* Corresponding author. Department of Orthopedic Surgery, Shanghai Jiao Tong University Affiliated Sixth People's Hospital, Shanghai, PR China.
** Corresponding author.
E-mail addresses: biyurui@aliyun.com (B. Rui), gangli@cuhk.edu.hk (G. Li).
[1] Jia Xu and Junjie Shen contributed equally to this work and are co-first authors.
[2] Biyu Rui and Gang Li contributed equally to this work

https://doi.org/10.1016/j.jot.2022.09.001
Received 22 May 2022; Received in revised form 12 August 2022; Accepted 1 September 2022

2214-031X/© 2022 Published by Elsevier B.V. on behalf of Chinese Speaking Orthopaedic Society. This is an open access article under the CC BY-NC-ND license (http://creativecommons.org/licenses/by-nc-nd/4.0/).

bone defects and restore function [4,5]. Although tissue engineering has achieved a certain degree of success in the past decade, complete repair of bone defects and restoration of function are yet to be achieved. One leading obstacle for most tissue-engineered scaffolds is the lack of sufficient vascularization within the scaffold [6]. As slow ingrowth of the host's vasculature into the center of bone grafts hinders further bone consolidation [7], some have concluded that neovascularization is vital to bone regeneration [8]. New strategies are needed to overcome this roadblock and effectively achieve vascularized tissue-engineered bone grafts.

One strategy that has gained much attention is using grafts that have been prevascularized *in vitro* or *in vivo*. Implantation of prefabricated vascular networks greatly expedites host vessel perfusion and facilitates tissue repair [9]. *In vivo* prevascularization approaches have several advantages over *in vitro* approaches, which are complex and labor intensive. Currently, various *in vivo* approaches are in use, including periosteal flap coverage, arteriovenous loop grafts, and vascular bundle insertion around or through grafts [10,11]. Basically, *in vivo* prevascularization strategies have been successfully employed in the repair of nerve tissue and large mandibular defects [12,13]. However, there are few studies that have investigated their use for repairing load-bearing extremities, and even fewer that have successfully developed and assessed degradable scaffolds capable of undergoing robust prevascularization and promoting subsequent angiogenesis and osteogenesis when applied to large bone defects. Thus, there is still room for the development and optimization of prevascularized bioreactors and appropriate scaffolds.

Since bone is mainly composed of apatitic calcium phosphate mineral, ceramic-based bone graft substitutes, such as beta-tricalcium phosphate (β-TCP), have been most extensively used [14]. Several studies demonstrated that β-TCP has desirable osteotransductive, osteoinductive, and biocompatible properties [15,16]. As such, β-TCP has been widely used for repairing large bone defects in recent decades [14]. In order to improve their repair performance, numerous β-TCP composite materials have been developed, with the aim of endowing β-TCP with more biological and durable yet biodegradable properties [17–19]. Nonetheless, little evidence exists on whether the osteogenic ability of β-TCP can be enhβ-TCP scaffoldanced by prevascularization treatment.

We recently conducted a series of studies to evaluate the importance of angiogenesis in enhancing osteogenesis [20–22]. Along these lines, the current study aimed to evaluate an alternative *in vivo* prevascularization strategy in which selected macroporous β-TCP scaffolds were used to accelerate bone regeneration in large segmental defects. Our objectives were threefold: (1) to develop modified macroporous β-TCP scaffolds, (2) to assess the utility of muscle pouches adjacent to a tibia defect as *in vivo* bioreactors for the prevascularization of the β-TCP scaffolds, and (3) to test the ability of the vascularized scaffolds to integrate with the host's existing vessels in a rat tibia bone defect model.

2. Materials and methods

2.1. Fabrication and characterization of β-TCP scaffolds

Macroporous β-TCP scaffolds were fabricated by a modified template-casting method [23,24]. Commercially available β-TCP powder was mixed with carboxymethyl cellulose (25 wt%), surfactant, and dispersant in distilled water to prepare a β-TCP ceramic slurry, which was casted and shaped into a preformed template composed of paraffin beads in the reaction polyethylene wells of a 96-well culture plate (Corning, Tewksbury, MA, USA). Before the β-TCP ceramic slurry was cast, the paraffin mold was heated in a water bath at 50 °C for 3 min, and then dried in an oven at 40 °C for 2 h to ensure that the paraffin beads at the contact points were fully melted. When the interconnective paraffin mold was completely filled with β-TCP ceramic slurry, it was solidified by dehydration in ascending concentrations of ethyl alcohols. The solidified β-TCP scaffold was removed from the mold and sintered in an electric furnace at 1200 °C for 3 h. Sintering converted the scaffold's structure into a macroporous structure. We have checked phase transition of β-TCP scaffolds after sintering to ensure that α-TCP not generated.

The morphology and microstructure of porous β-TCP scaffolds were analyzed by scanning electron microscopy (SEM, JSM-5600; JEOL Ltd., Tokyo, Japan) at an accelerator voltage of 20 kV. Samples were prepared by coating the scaffold with a 5-nm-thick Pt–Au film prior to microscopy. The scaffolds in this study measured approximately 4 mm in diameter and 5 mm in length.

2.2. In vivo prevascularization and animal surgery

All procedures were approved by the Animal Research Committee of Prince of Wales Hospital of the Chinese University of Hong Kong (No. 14-052-MIS). All procedures were approved by the Animal Research Committee of our hospital (No. 14-052-MIS). The animal experiments were performed in accordance with relevant guidelines and regulations [25]. A total of 72 male Sprague–Dawley rats (300–350 g) were randomly assigned to a prevascularized macroporous β-TCPs group (vascularization group, n = 36, equally divided into 9 rats at each termination) and a non-prevascularized macroporous β-TCPs group (blank group, n = 36, equally divided into 9 rats at each termination). For the *in vivo* prevascularization procedure, we chose the muscle adjacent to the lateral thigh as the bioreactor site for prevascularization of the scaffolds. Macroporous β-TCP scaffolds were carefully embedded within a muscle pouch created within the vastus lateralis muscle and it remained there for 3 weeks, which was enough time for a microvascular network to form and penetrate the pores of the construct. Three weeks after implantation, the prevascularized macroporous β-TCP scaffolds were harvested and then implanted in the tibia defect. β-TCP scaffolds not implanted into the bioreactor muscle served as blank controls.

2.3. Segmental tibia defect model

The segmental tibia bone defect model was established according to the protocol we described previously [21]. Briefly, a total of 72 rats were anesthetized with pentobarbital, the right tibia was exposed, and a mid-diaphysis transverse osteotomy was performed at the midshaft level to create a 5-mm-wide defect producing two bone segments. Next, a unilateral external fixator (Xinzhong Medical Devices Co., Ltd., Tianjin, China) was mounted onto the bone segments with four stainless steel pins in order to fix the proximal and distal tibia segments in place. Prevascularized (n = 36) or blank (n = 36, non prevascularized, set as the control group). β-TCPs scaffolds were then implanted into the tibia defect (i.e., between the two bone segments). The rats were sacrificed 2, 4, 6, or 8 weeks after implantation surgery. The timeline of events is shown in Fig. 1B. The sample sizes were selected to enable evaluation of statistical significance of difference between groups. Randomisation was used to allocate experimental units. The rats were selected in random order from one of the 24 cages in order to minimize potential confounders such as cage location. Rats were excluded due to death during the procedure or failing to meet the exclusion/inclusion criteria. Researchers performing animal experiments were not blinded.

2.4. Digital radiography

Animals underwent anterior-posterior X-rays 2, 4, 6, and 8 weeks (n = 9 at each time point) after implantation surgery using a digital X-ray machine (MX-20, Faxitron X-Ray Corp., Wheeling, IL, USA) at an exposure time of 6000 ms and a voltage of 32 kV. The rats were anesthetized under general anesthesia during the X-rays.

2.5. Micro-computed tomography

The rats (n = 3 per group at each time termination) underwent micro-computed tomography (micro-CT) in order to detect structural changes

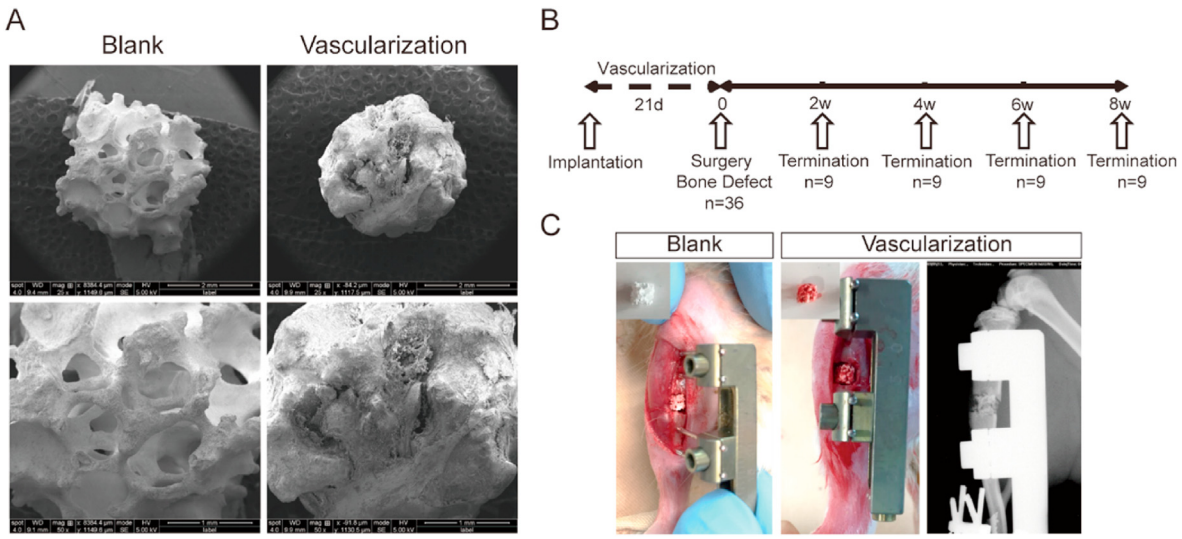

Figure 1. Prevascularized macroporous beta-tricalcium phosphate (β-TCP) scaffolds were used to treat a segmental tibia defect in rat (A) Scanning electron micrographs showing the structure of β-TCP scaffolds before (blank) and after *in vivo* prevascularization (B) Overall schematic diagram illustrating the study design. After implantation into the tibia defect, the prevascularized scaffolds were assessed at the indicated weeks. (C) Photographs showing the positions of blank and vascularized macroporous β-TCP scaffolds implanted into a segmental tibia defect. Far right panel shows an X-ray radiograph of the position of the vascularized macroporous β-TCP scaffold in the bone defect.

in the newly formed callus and mineralized bone. Eight weeks after scaffold implantation, the rats were sacrificed with an overdose of pentobarbital anesthesia and their tibias were harvested. Samples were assessed with high-solution micro-CT (SkyScan-1176; Bruker Corporation, Billerica, MA, USA) using different thresholds. The machine was set to a voltage of 70 kV and a current of 114 μA. Three-dimensional (3D) reconstructions of mineralized callus were generated by Gaussian filtering (sigma = 0.8 and support = 2) at the global threshold (165 mg hydroxyapatite/cm^3). Regenerated bone site was selected as the region of interest (ROI), low- and high-density mineralized tissues were reconstructed using different thresholds (low attenuation = 158, high attenuation = 211) using our established evaluation protocol [26]. Higher density tissues represented the newly formed highly mineralized calluses while the low-density tissues represented the newly formed calluses. Bone volume/total tissue volume (BV/TV), connected density (Conn-Dens), Tb. Sp (trabecular separation), Tb.N (trabecular number), Tb.Th (trabecular thickness), and bone mineral density (BMD) were analyzed using CTAN software (Skyscan, Bruker Corporation, Billerica, MA, USA) and CTvol software packages (Skyscan, Bruker Corporation, Billerica, MA, USA).

To assess and compare neovascularization during bone regeneration, we performed angiography on anesthetized rats 2, 4, 6, and 8 weeks after implantation surgery. Briefly, the rats were intracardially perfused through the left ventricle with 4% paraformaldehyde (PFA) followed by Microfil MV122 injection compound (Flow Tech, Inc., Carver, MA, USA), a silicone rubber compound commonly used to fill vasculature postmortem. Then the callus within the defect was subjected to high-resolution micro-CT with an isometric scanning layers thickness of 9 μm. The vascular network was reconstructed in 3D using CTAN software.

2.6. Biomechanical test

Eight weeks after scaffold implantation, the mechanical strength of the repaired tibia specimens was assessed. We tested for tibia failure along the anterior-posterior plane using a four-point bending device (H25KS; Hounsfield Test Equipment, Surrey, UK) with a 250-N load cell applied to the tibia. The inner and outer span of the blades were set to 8 and 18 mm, respectively. The long axis of the tibia was oriented perpendicular to the blades during testing. A load was continuously applied to the defect zone at a displacement rate of 5 mm/min. The modulus of elasticity (E-modulus), ultimate load, energy to failure, and maximum stress were recorded with QMAT Professional software (Tinius Olsen, Horsham, PA, USA). Contralateral tibias were similarly tested and served as internal controls.

2.7. Histological and immunohistochemical analyses

Regenerated tibia samples (n = 3 per group at each time termination) were harvested 2, 4, 6, and 8 weeks after scaffold implantation and submersion fixed in 4% PFA for 3 days. The samples were then dehydrated in graded concentrations of alcohols, and then decalcified with 10% EDTA for 6 weeks. The samples were then embedded in paraffin and sectioned into 5-μm-thick sections along the long axis in the midsagittal plane. For histological analyses, sections were stained with hematoxylin-eosin (HE) and Masson's trichrome stains. For immunohistochemical (IHC) staining, the sections were incubated in primary antibodies against CD31, CD34, VEGF-A, or osteocalcin (OCN) (1:200; Abcam, Cambridge, UK) overnight at 4 °C, followed by species-appropriate HRP-conjugated secondary antibodies (1:1000, Jackson Research). Immunoreactivity was visualized with 3,3′-diaminobenzidine (DAB). Integrated optical density (IOD) was measured in five randomly selected visual fields per section using ImageJ software (National Institutes of Health, Bethesda, MD, USA).

2.8. Real-time quantitative RT-PCR analyses

Osteogenesis and angiogenesis in bone defects receiving scaffold implants were assessed by measuring the expression levels of two growth factors (bone morphogenetic protein 2 [BMP2] and vascular endothelial growth factor A [VEGF-A]) 2, 4, 6, and 8 weeks (n = 3 per group at each time termination) after scaffold implantation. Total RNA was extracted from the collected specimens using TRIzol® (Life Technologies, Carlsbad, CA, USA) and after homogenization with liquid nitrogen. Isolated RNA was reverse-transcribed with PrimeScript RT Reagent Kit (Takara, Kusatsu, Shiga, Japan). The housekeeping gene GAPDH served as the internal control for normalization. The control group represents the normal bone. The primer sequences were as follows: BMP2 forward: 5-AAGCCAAACACAAACAGCGG-3, reverse: 5-TTCTCCGTGGCAGTAAAAGGC -3; VEGF-A forward: 5-ACCTCATGCTGATACCGGGTCC-3, reverse: 5-CCGGGGCGTGGAG-TACCTGT-3.

2.9. Western blot analyses

At 2, 4, 6, and 8 weeks (n = 3 per group at each time termination) after scaffold implantation, bone tissue specimens were homogenized in RIPA (Bio-Rad, Hercules, CA, USA) supplemented with protease inhibitor. After incubation at 4 °C for 30 min, the specimens underwent centrifugation at 14,000 rpm for 15 min. Protein concentration was measured with a BCA protein assay kit (Thermo, Rockford, MD, USA). Protein samples were subjected to 10% (w/v) SDS-PAGE, and separated proteins were transferred onto polyvinylidene difluoride membranes (Millipore, Billerica, MA, USA). After blocking with 7% skim milk, the membranes were incubated overnight at 4 °C with primary antibodies against BMP2 and VEGFA (1:2000; Abcam, Cambridge, UK), and then incubated with secondary antibody (Cell Signaling Technology®, Beverly, MA, USA) at room temperature for 1 h. The bands were captured using an imaging system (ImageQuant™ LAS 4000 mini, GE Healthcare Life Sciences, Chicago, USA), and then semi-quantified using ImageJ software (National Institutes of Health, Bethesda, MD, USA).

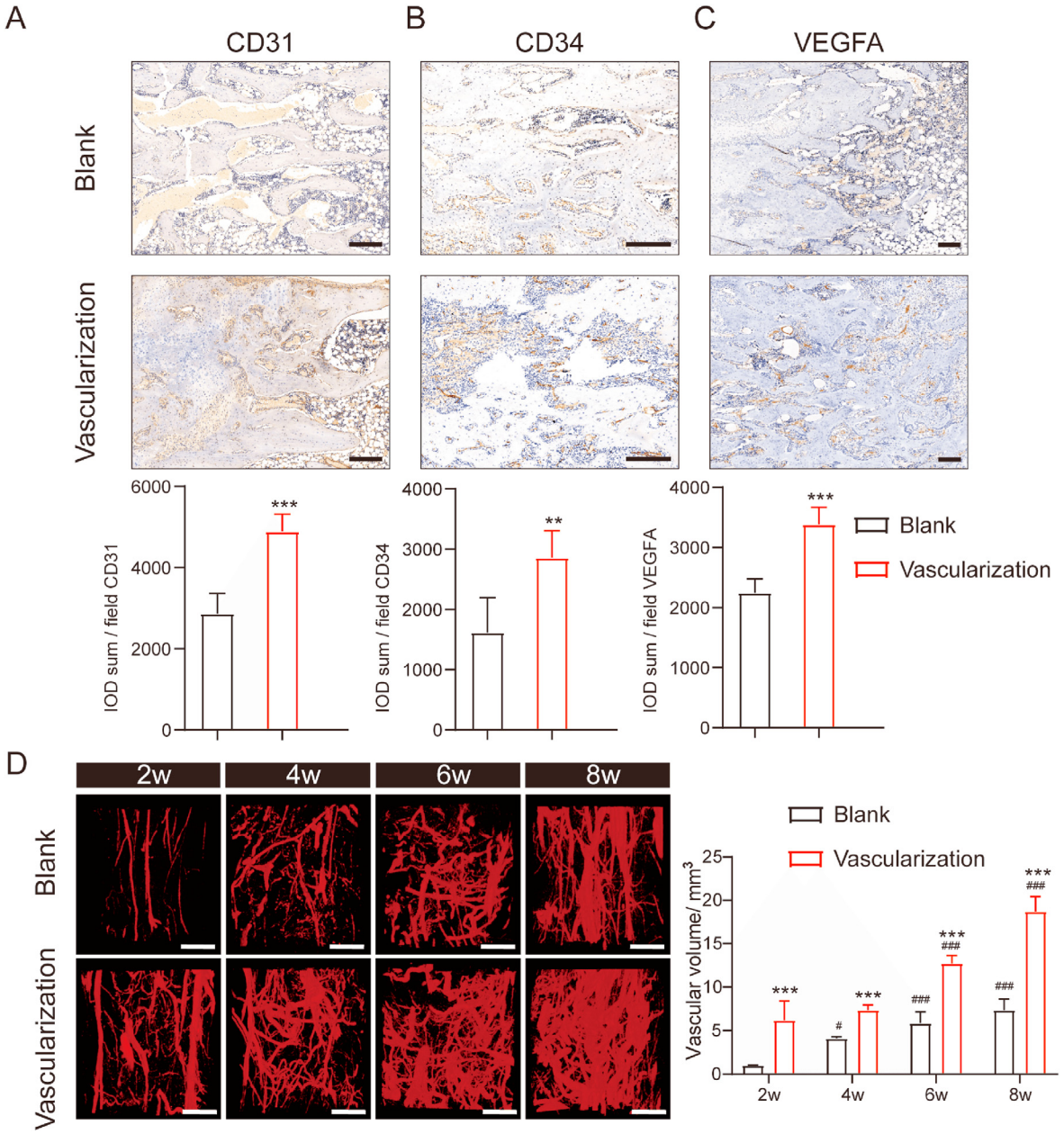

Figure 2. Vascular formation was accelerated in rats with prevascularized macroporous β-TCP scaffolds in thesegmental tibial bone defect (A–C) Representative and quantitative analysis of CD31-, CD34-, and VEGF-A-immunostained sections from rats implanted with a blank or prevascularized b-TCP scaffold. The rats underwent consolidation for 8 weeks. Scale bars, 200 μm n = 3 in each group. *p < 0.05; **p < 0.01; and ***p < 0.001 (D) Representative micro-CT images of the vessel network within regenerating bone in rats with a tibia bone defect at 2, 4, 6, and 8 weeks after implantation with a blank or prevascularized b-TCP scaffold. Scale bars, 1 mm. Two-way ANOVA with the Bonferroni post hoc test was used to determine significant differences among groups. n = 3 in each group. ***p < 0.001 for the vascularization group vs the blank group in each week; #p < 0.05 and ###p < 0.001 for 4, 6, and 8 weeks vs 2 week in each group.

2.10. Statistical analyses

Quantitative results were presented as means ± standard deviations and analyzed with SPSS 22.0 software (IBM Corp. Released 2013, Armonk, NY: IBM Corp.). Two-tailed Student's t test was used to evaluate statistical differences, and a p value of <0.05 was considered statistically significant.

3. Results

3.1. Morphology of in vivo prevascularized macroporous β-TCP scaffolds

Prior to assessing the angiogenic and osteogenic potential of β-TCP scaffolds, we first evaluated the structure of blank/non-vascularized and prevascularized scaffolds at the macroscopic and SEM levels (Fig. 1A, C). As shown in Fig. 1A, the scaffold's macropores were highly interconnected; this network of interconnected macropores facilitated nutrient permeability and vessel ingrowth. Despite being implanted for 3 weeks within a muscle pouch and undergoing prevascularization, the β-TCP scaffold's structure remained intact and retained its porous structure (Fig. 1A). During *in vivo* prevascularization, the scaffold's macropores achieved a desirable level of vascularization and were sufficiently infiltrated by supporting fibrous components.

3.2. In vivo prevascularization of scaffolds promoted angiogenesis

To determine to what extent prevascularization of scaffolds affects vessel formation in and around segmental tibia bone defects, we implanted blank or prevascularized scaffolds between the two bone segments and assessed vessel formation 2, 4, 6, and 8 weeks later via IHC. Abundant vessel formation was observed in the vascularization group at each of the indicated time points. Immunostaining for endothelial cell markers (CD31, CD34, VEGFA) showed that CD31 and CD34 staining was denser and more widely distributed in tissue sections from the vascularization group than those from the blank group (Fig. 2A–C). Similarly, immunostaining for VEGF-A, a master regulator of angiogenesis [27], appeared to be more robust in the vascularization group than in the blank group. This is consistent with our observation that in the prevascularized group, prevascularized bone scaffolds increased the amount and density of capillaries surrounding regenerated bone.

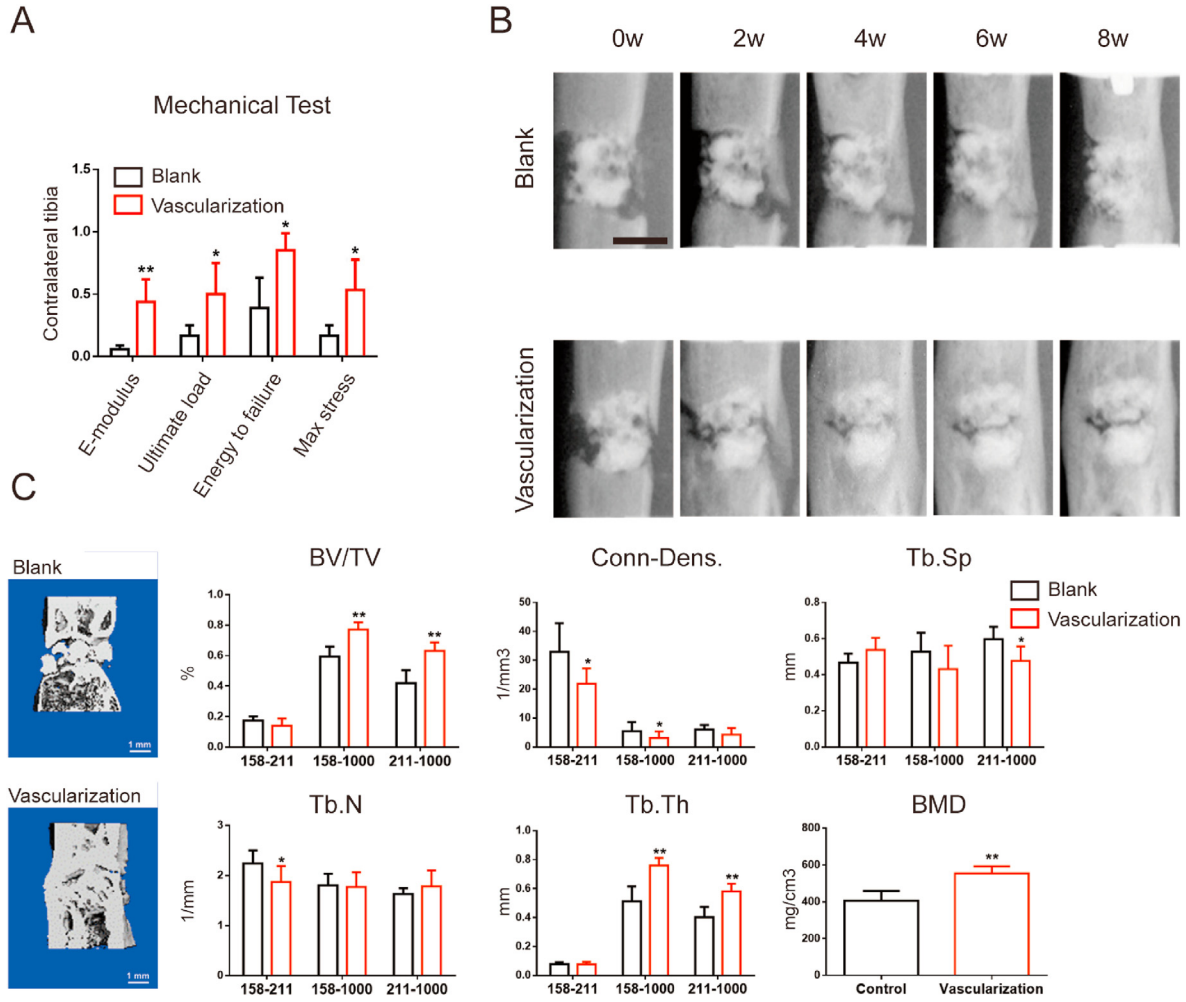

Figure 3. Prevascularized macroporous β-TCP scaffolds accelerated bone consolidation during osteogenesis in rats with a segmental tibial defect (A) Mechanical properties (E-modulus, ultimate load, energy to failure, and max stress) of the site in and around the tibial defect 8 weeks after implantation of a blank or prevascularized scaffold. The values were normalized to the corresponding contralateral normal tibias. n = 3 in each group (B) Representative X-ray images (lateral view) of the bone defect after 0, 2, 4, 6, and 8 weeks of consolidation. Bright white angular area represents the metal unilateral external fixator. n = 9 in each group. Scale bar, 5 mm (C) Three-dimensional reconstructions of micro-CT images after 8 weeks of consolidation (left panels) and histograms showing different mechanical parameters of bone tissue mineralization at the indicated indices measured at three different thresholds. Attenuation above 158 represents total mineralized tissue, and attenuation between 158 and 211 represents the newly formed calluses. n = 3 in each group. BV/TV, bone volume/tissue volume; Conn-Dens, connectivity density; Tb.Sp, trabecular separation; Tb.N, trabecular number; Tb.Th, trabecular thickness; BMD, bone mineral density. Significant differences were evaluated by Student's t tests; *p < 0.05; **p < 0.01.

As perfusion determines the final outcome of bone grafts [28], next we determined whether the newly formed vessels supported adequate blood perfusion within the regenerated bone by perfusing the rats with Microfil, a silicone rubber contrast agent frequently used in vascular research [29], and then imaging the vasculature via micro-CT. Three--dimensional reconstructions of the imaged vessels showed that functional vascular networks formed more quickly in the vascularization group (Fig. 2D). During early stages of angiogenesis, we observed large vessels branching into smaller ones, which ultimately developed into a complex and well-defined network of vessels. This process was not apparent in the blank group (Fig. 2D).

3.3. Prevascularized β-TCP scaffolds accelerated bone consolidation

We assessed the effects of implantation of prevascularized β-TCP scaffolds compared to blank scaffolds on bone consolidation by measuring the mechanical properties of respective tibia specimens over time. The vascularization group showed significantly better values on E-modulus, ultimate load, energy to failure, and max stress parameters than did the blank group (Fig. 3A). Longitudinal X-ray views of the of the defect site 2, 4, 6, and 8 weeks after implantation revealed that, at each time point, bone consolidation was more robust in the vascularization group, showing a greater volume of newly mineralized cortex, than that in the blank group (Fig. 3B). At the final time point, more calluses were observed in the vascularization group than in the blank group (Fig. 3B). This is clearly shown in 3D reconstructions of regenerated bone 8 weeks after implantation surgery (Fig. 3C). In the vascularization group, BV/TV and Tb.Th values were considerably greater at the 158–1000 and 211–1000 thresholds than those in the blank group. BMD values were also higher in the vascularization group than in the blank group, indicating that the prevascularized β-TCP scaffolds had accelerated bone consolidation.

3.4. In vivo prevascularized scaffolds enhanced vascularization of regenerated bone

To determine to what extent prevascularization of a scaffold enhances vascularization of regenerated bone, we analyzed vascular networks in tissue sections from the regenerated bone 2, 4, 6, and 8 weeks after implantation of blank or prevascularized β-TCP scaffolds at a segmental tibia defect. During the consolidation phase, the center of the defect site became inundated with a zone of fibers rich in chondrocyte-like cells as the callus was being stretched (Fig. 4A and B). At 4 and 6 weeks after scaffold implantation in the vascularization group, HE and Masson's trichrome staining revealed newly formed trabecular bone and columns of cartilaginous tissues. At 8 weeks, the vascularization group exhibited faster bone marrow recanalization than the blank group. Similarly, OCN staining was much denser and more extensively distributed in sections from the vascularization group, indicating higher OCN expression and more active osteogenesis (Fig. 5A and B). To further investigate angiogenesis and osteogenesis activity, we measured the expression of BMP2 and VEGF-A by quantitative RT-PCR and western blotting. BMP2 and VEGF-A mRNA levels in the vascularization group were significantly higher than those in the blank group 2, 4, and 6 weeks after implantation, with the peak expression occurring 2 weeks after implantation (Fig. 5C). These findings were corroborated by western blotting, which showed that BMP2 and VEGF-A protein expression was higher after *in vivo* prevascularization treatment and implantation (Fig. 5D–F). Collectively, these results provide supporting evidence that the *in vivo* prevascularization strategy contributed to the enhancement of vascularized bone regeneration.

4. Discussion

In the present study, we used a relatively efficient, clinical prevascularization method combined with classic macroporous β-TCP scaffolds to enhance bone regeneration in a segmental tibia defect model in rat. In this method, the scaffold is inserted into a muscle pouch adjacent to the defect, where it remains for 3 weeks to allow for vascularization. Once vascularized, the scaffold is transferred to the defect site. We found that this *in vivo* prevascularization strategy enhanced the angiogenic properties of macroporous β-TCP scaffolds, thus promoting bone regeneration. The rationale for prevascularizing the scaffolds in muscle derived from the premise that muscle tissue has a rich blood supply and thus is ideal for prevascularization of scaffolds [30]. During *in vivo* prevascularization, vessels in the muscle pouch surrounding the scaffold penetrated the pores of the scaffolds, making this strategy particularly useful for bone repair applications. Also, this strategy was practical and feasible for use in long-bone defects. In vivo prevascularization is a more clinically translatable method, as it uses the body's environment to promote host vascular network ingrowth inside the scaffold. We found that, when used for our *in vivo* prevascularization, interconnected vascular networks formed in a more spatiotemporally controlled manner.

Our present IHC and angiography results revealed that over time, the density and distribution of vessels were greater in rats that had received the prevascularized scaffold (prevascularized group) than those that

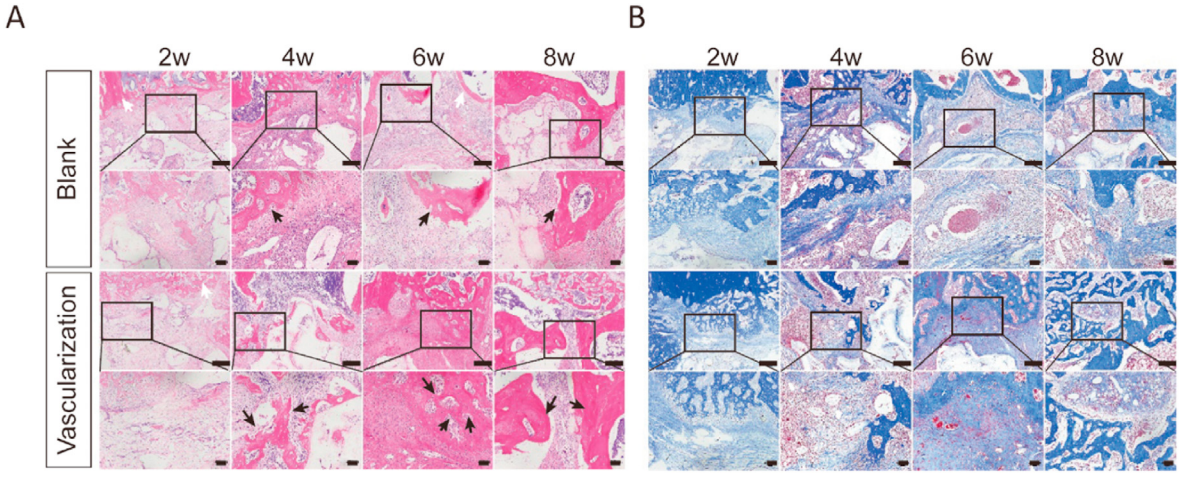

Figure 4. *In vivo* prevascularized macroporous β-TCP scaffold enhanced bone regeneration within the tibial defect site (A, B) Regenerated bone tissue in histological sections through the segmental tibia defect of rats implanted with either a blank or prevascularized scaffold. The sections were stained with hematoxylin and eosin (A) or Masson's trichrome stain (B) 2, 4, 6, and 8 weeks after implantation. New generated bone is marked with arrows in black and host bone tissue with white arrows in HE staining. n = 3 in each group. Higher magnification photographs of boxed areas are shown in the subjacent panels. Scale bars, 400 μm.

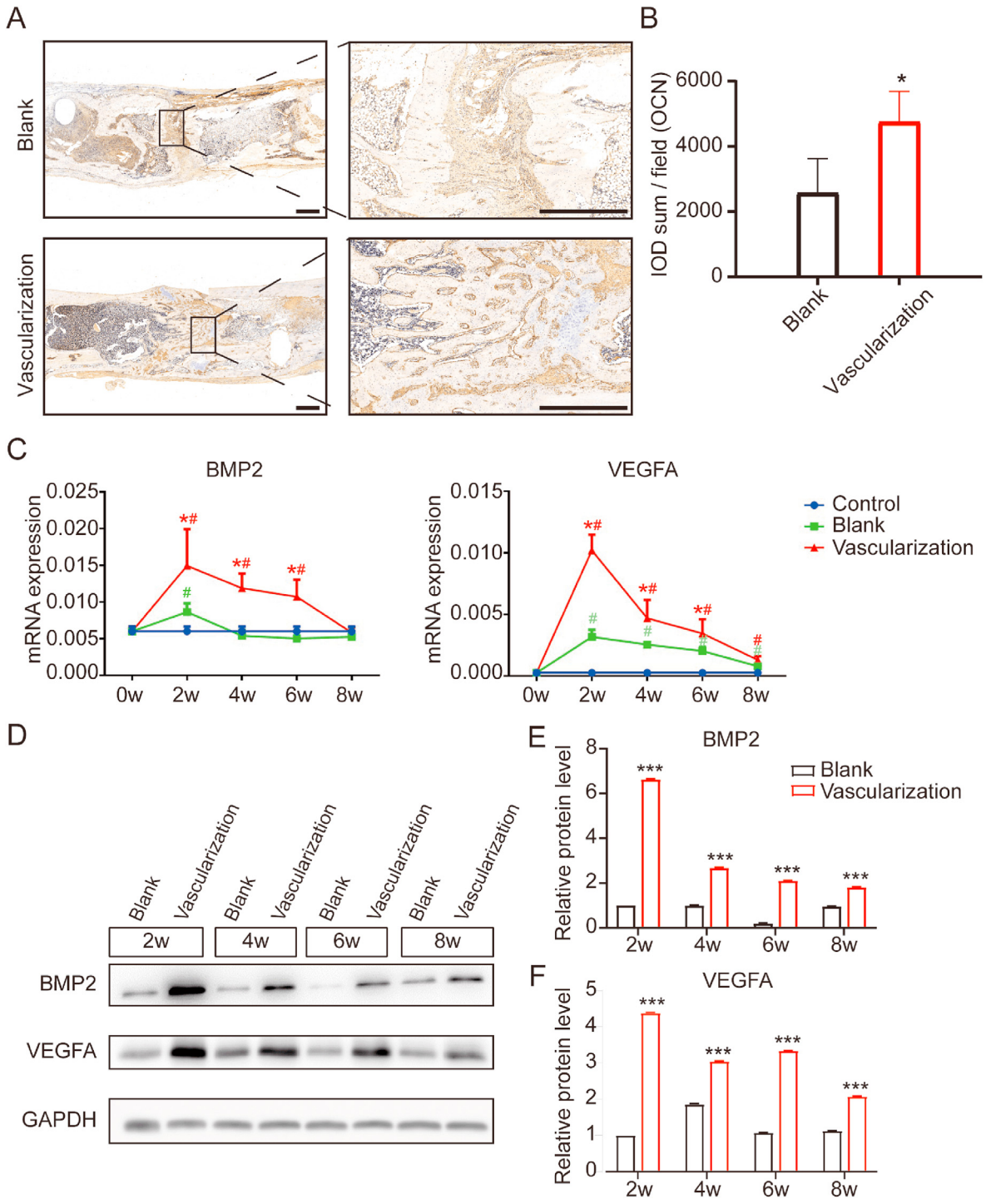

Figure 5. *In vivo* prevascularized scaffold enhanced vascularization of regenerated bone within a segmental tibial defect in rats (A) Tissue sections through the segmental tibia defect immunostained for osteocalcin (OCN), a hormone secreted by osteoblasts. These sections were taken from rats 8 weeks after implantation with either a blank or prevascularized scaffold. Higher magnification photograph of boxed areas are shown to the right. Scale bars, 1000 μm n = 3 in each group (B) Integrated optical density (IOD) of OCN-positive staining in tissue sections from rats 8 weeks after implantation of scaffold (C) BMP2 and VEGFA mRNA expression levels in regenerated bone tissue 2, 4, 6, and 8 weeks after implantation of scaffold. Expression was quantified by RT-PCR. The housekeeping gene GAPDH served as an internal control. n = 3 in each group. (D) Western blots of lysates derived from regenerated bone tissue at the indicated times after implantation. n = 3 in each group. (E, F) Quantification of BMP2 and VEGFA protein expression levels in regenerated bone tissue at the indicated times after implantation of scaffold. Expression was evaluated by western blotting. The housekeeping gene GAPDH served as an internal control. Significant differences were evaluated by Student's t tests; *$p < 0.05$; **$p < 0.01$; ***$p < 0.001$, compared with the blank group. $^{\#}p < 0.05$, compared with the control.

received a non-vascularized scaffold (blank group). This demonstrated that the vessels in the prevascularized scaffold had connected successfully to the host's capillaries, providing the regenerated bone with a functional blood supply, which is consistent with the findings of a previous study [31]. The enhanced angiogenesis we observed was corroborated by RT-PCR and western blot analyses showing that the expression of the angiogenesis marker VEGFA significantly increased in the first 2 weeks after implantation of the prevascularized scaffold. This

also demonstrated that prevascularizing the scaffolds significantly improved their angiogenic ability, as VEGFA expression in samples from control animals was very low (cf. Fig. 5). VEGF has been proven to promote the angiogenesis of endothelial cells during endochondral bone osteogenesis [32].

In the present study, we also observed that the prevascularized scaffolds enhanced osteogenesis. Mechanical, X-ray, and micro-CT analyses of newly regenerated bone showed that bone tissue mineralization was significantly greater in rats in the prevascularization group than in the blank group. A previous study, however, found that β-TCPs performed poorly when used to repair a segmental bone defect in rabbit humerus [33]. One possible explanation for these disparate results may be that the scaffold they implanted into the defect was insufficiently vascularized. In the present study, the intramuscular prevascularization strategy produced a robustly vascularized β-TCP scaffold capable of promoting angiogenesis and subsequent osteogenesis at the defect site. This was verified by IHC for OCN, a hormone secreted by osteoblasts, and RT-PCR and western blot analyses for BMP2, an osteogenic marker.

Repairing large segmental bone defects remains to be a significant challenge in clinical practice. One dominant factor contributing to this challenge is achieving adequate vascularization within the defect site. Adequate vascularization is prerequisite to achieving satisfactory bone regeneration and favorable outcome, as angiogenesis and osteogenesis are significantly and positively correlated [7,34]. The development of tissue engineering, biotechnology, and microsurgery techniques has made it possible to achieve adequate vascularization in large bone defects. Prevascularization methods have become important for constructing vasculature to facilitate tissue repair and regeneration. Several researchers have analyzed the quality and quantity of vascular bundles that invade the grooves of various scaffolds, with or without growth factors and stem cells [35,36]. When implanted into the bone defect, the vasculature within these scaffolds behaved similarly to those within vascularized autologous bone grafts, in which the vessels of harvested bone grafts were anastomosed with the local vasculature at the defect site. Although this vascular bundle technique is efficient, and with continued improvement, it is too costly and too technically demanding for clinical translation. In addition, bundle stability after transplantation cannot be ensured. Those studies, however, laid the groundwork for our *in vivo* prevascularization strategy.

In the present study, our aim was to develop a cost-effective, relatively simple strategy to vascularize a scaffold *in vivo*. The rationale behind our strategy was similar to the *in vitro* seeding of endothelial cells onto the surface of scaffolds, where microvascular-like structures are subsequently formed and transferred to a defect site [37,38]. These *in vitro* procedures, however, are more complicated and time-consuming than our method, and the microvascular-like structures formed are less robust, failing to fully arborize and extend into the pores of the scaffolds. Our strategy addressed these limitations by using the recipient's own muscle as an *in vivo* bioreactor, where the scaffold can be implanted temporarily and undergo prevascularization before being transferred to the defect site. In our strategy, the resulting vasculature is robust, infiltrating the pores of the scaffold, and most of the vessel architecture is preserved upon transfer to the defect. These features favor *in vivo* prevascularization for possible use in future clinical applications.

Although angiogenesis and osteogenesis appeared to be coupled, the mechanism of this intercellular crosstalk and the role of tissue engineering remained undetermined. During bone regeneration process, besides osteoblasts and osteoclasts, endothelial cells and mesenchymal stem cells (MSCs) also participated in bone formation and remodeling [39]. Accumulating evidence indicated that several signaling pathways are potentially activated, including Notch signaling, VEGFR2-related signaling, and AKT signaling [39,40]. It is reported that sustained release of nanoparticles such as PLGA/β-TCPs increased MSCs recruitment and osteogenic differentiation, further activating the coupling of angiogenesis-to-osteogenesis [41]. The porosity structure and prevascularization technique might accelerate tissue engineering mediating the physiological process of bone regeneration [42]. Our *in vivo* prevascularization of microporous β-TCP scaffolds produced a functional vascular supply for regenerated bone within a segmental bone defect, subsequently leading to bone mineralization and repair. Our results were subject to some limitations. Because of the material property, observation of the prevascularized β-TCP scaffolds was only achieved by SEM and morphology observation. Besides, we did not investigate the detailed mechanisms underlying scaffold-associated angiogenesis and subsequent osteogenesis. These mechanisms remain elusive and requires further research.

5. Conclusion

The present study introduced a novel *in vivo* prevascularization strategy for growing vasculature on scaffolds to be used for repair of large segmental bone defects. *In vivo* prevascularized β-TCP scaffolds are superior in many aspects to other methods in that their vascular supply is robust, has superior mechanical integrity, and leads to faster bone regeneration. These characteristics make prevascularized tissue-engineered bone grafts promising for use in clinical applications.

Data availability statement

The datasets used and/or analyzed during the current study are available from the corresponding author on reasonable request.

Author contributions

GL and BR conceived and designed the experiments. JX and JS performed the experiments and wrote the manuscript. YS, TW, and YS analyzed the data. YC and QK prepared all the figures. All the authors reviewed and agreed upon the final version of this manuscript.

Ethical statement

Overall animal experimental designs and schemes were approved by the Animal Research Committee of Prince of Wales Hospital of the Chinese University of Hong Kong (No. 14-052-MIS).

Funding

This work was sponsored by grants from the Basic Research Project of Shanghai Sixth People's Hospital (General Cultivation Project, ynms202104) to JX; National Natural Science Foundation of China (81930069) and Major Scientific Research and Innovation Project of Shanghai Municipal Education Commission (2019-01-07-00-02-E00043) to YC.

Declaration of competing interest

The authors declare that they have no known competing financial interests or personal relationships that could have appeared to influence the work reported in this paper.

Acknowledgments

Not applicable.

References

[1] Yang YP, Gadomski BC, Bruyas A, Easley J, Labus KM, Nelson B, et al. Investigation of a prevascularized bone graft for large defects in the ovine tibia. Tissue Eng 2021; 27(23–24):1458–69.

[2] Dheenadhayalan J, Devendra A, Velmurugesan P, Shanmukha Babu T, Ramesh P, Zackariya M, et al. Reconstruction of massive segmental distal femoral metaphyseal bone defects after open injury: a study of 20 patients managed with intercalary

gamma-irradiated structural allografts and autologous cancellous grafts. J Bone Joint Surg Am 2022;104(2):172–80.
[3] Vidal L, Brennan MA, Krissian S, De Lima J, Hoornaert A, Rosset P, et al. In situ production of pre-vascularized synthetic bone grafts for regenerating critical-sized defects in rabbits. Acta Biomater 2020;114:384–94.
[4] Kim HD, Amirthalingam S, Kim SL, Lee SS, Rangasamy J, Hwang NS. Biomimetic materials and fabrication approaches for bone tissue engineering. Adv Healthc Mater 2017;6(23).
[5] Xu G, Hu X, Han L, Zhao Y, Li Z. The construction of a novel xenograft bovine bone scaffold, (DSS)6-liposome/CKIP-1 siRNA/calcine bone and its osteogenesis evaluation on skull defect in rats. J Orthop Translat 2021;28:74–82.
[6] Yin S, Zhang W, Zhang Z, Jiang X. Recent advances in scaffold design and material for vascularized tissue-engineered bone regeneration. Adv Healthc Mater 2019;8(10):e1801433.
[7] Filipowska J, Tomaszewski KA, Niedzwiedzki L, Walocha JA, Niedzwiedzki T. The role of vasculature in bone development, regeneration and proper systemic functioning. Angiogenesis 2017;20(3):291–302.
[8] Ranmuthu CDS, Ranmuthu CKI, Russell JC, Singhania D, Khan WS. Evaluating the effect of non-cellular bioactive glass-containing scaffolds on osteogenesis and angiogenesis in in vivo animal bone defect models. Front Bioeng Biotechnol 2020;8:430.
[9] Simunovic F, Finkenzeller G. Vascularization strategies in bone tissue engineering. Cells 2021;10(7).
[10] Beier JP, Horch RE, Hess A, Arkudas A, Heinrich J, Loew J, et al. Axial vascularization of a large volume calcium phosphate ceramic bone substitute in the sheep AV loop model. J Tissue Eng Regen Med 2010;4(3):216–23.
[11] Wang L, Fan H, Zhang ZY, Lou AJ, Pei GX, Jiang S, et al. Osteogenesis and angiogenesis of tissue-engineered bone constructed by prevascularized beta-tricalcium phosphate scaffold and mesenchymal stem cells. Biomaterials 2010;31(36):9452–61.
[12] Shen J, Wang J, Liu X, Sun Y, Yin A, Chai Y, et al. In situ prevascularization strategy with three-dimensional porous conduits for neural tissue engineering. ACS Appl Mater Interfaces 2021;13(43):50785–801.
[13] Tatara AM, Wong ME, Mikos AG. In vivo bioreactors for mandibular reconstruction. J Dent Res 2014;93(12):1196–202.
[14] Bohner M, Santoni BLG, Dobelin N. beta-tricalcium phosphate for bone substitution: synthesis and properties. Acta Biomater 2020;113:23–41.
[15] Damron TA. Use of 3D beta-tricalcium phosphate (Vitoss) scaffolds in repairing bone defects. Nanomed. 2007;2(6):763–75.
[16] Yuan H, Fernandes H, Habibovic P, de Boer J, Barradas AM, de Ruiter A, et al. Osteoinductive ceramics as a synthetic alternative to autologous bone grafting. Proc Natl Acad Sci U S A 2010;107(31):13614–9.
[17] Cao H, Kuboyama N. A biodegradable porous composite scaffold of PGA/beta-TCP for bone tissue engineering. Bone 2010;46(2):386–95.
[18] Kon E, Salamanna F, Filardo G, Di Matteo B, Shabshin N, Shani J, et al. Bone regeneration in load-bearing segmental defects, guided by biomorphic, hierarchically structured apatitic scaffold. Front Bioeng Biotechnol 2021;9:734486.
[19] Zhang D, Gao P, Li Q, Li J, Li X, Liu X, et al. Engineering biomimetic periosteum with beta-TCP scaffolds to promote bone formation in calvarial defects of rats. Stem Cell Res Ther 2017;8(1):134.
[20] Liu X, Sun Y, Shen J, Min HS, Xu J, Chai Y. Strontium doped mesoporous silica nanoparticles accelerate osteogenesis and angiogenesis in distraction osteogenesis by activation of Wnt pathway. Nanomedicine 2022;41:102496.
[21] Shen J, Sun Y, Liu X, Zhu Y, Bao B, Gao T, et al. EGFL6 regulates angiogenesis and osteogenesis in distraction osteogenesis via Wnt/beta-catenin signaling. Stem Cell Res Ther 2021;12(1):415.
[22] Sun Y, Liu X, Zhu Y, Han Y, Shen J, Bao B, et al. Tunable and controlled release of cobalt ions from metal-organic framework hydrogel nanocomposites enhances bone regeneration. ACS Appl Mater Interfaces 2021;13(49):59051–66.
[23] Kang Y, Ren L, Yang Y. Engineering vascularized bone grafts by integrating a biomimetic periosteum and beta-TCP scaffold. ACS Appl Mater Interfaces 2014;6(12):9622–33.
[24] Liu Y, Kim JH, Young D, Kim S, Nishimoto SK, Yang Y. Novel template-casting technique for fabricating beta-tricalcium phosphate scaffolds with high interconnectivity and mechanical strength and in vitro cell responses. J Biomed Mater Res 2010;92(3):997–1006.
[25] Percie du Sert N, Ahluwalia A, Alam S, Avey MT, Baker M, Browne WJ, et al. Reporting animal research: explanation and elaboration for the ARRIVE guidelines 2.0. PLoS Biol 2020;18(7):e3000411.
[26] Xu J, Wang B, Sun Y, Wu T, Liu Y, Zhang J, et al. Human fetal mesenchymal stem cell secretome enhances bone consolidation in distraction osteogenesis. Stem Cell Res Ther 2016;7(1):134.
[27] Ferrara N. Vascular endothelial growth factor: basic science and clinical progress. Endocr Rev 2004;25(4):581–611.
[28] Rouwkema J, Khademhosseini A. Vascularization and angiogenesis in tissue engineering: beyond creating static networks. Trends Biotechnol 2016;34(9):733–45.
[29] Zhang F, Qiu T, Wu X, Wan C, Shi W, Wang Y, et al. Sustained BMP signaling in osteoblasts stimulates bone formation by promoting angiogenesis and osteoblast differentiation. J Bone Miner Res 2009;24(7):1224–33.
[30] Warnke PH, Wiltfang J, Springer I, Acil Y, Bolte H, Kosmahl M, et al. Man as living bioreactor: fate of an exogenously prepared customized tissue-engineered mandible. Biomaterials 2006;27(17):3163–7.
[31] Laschke MW, Rucker M, Jensen G, Carvalho C, Mulhaupt R, Gellrich NC, et al. Improvement of vascularization of PLGA scaffolds by inosculation of in situ-preformed functional blood vessels with the host microvasculature. Ann Surg 2008;248(6):939–48.
[32] Ferrara N, Gerber HP, LeCouter J. The biology of VEGF and its receptors. Nat Med 2003;9(6):669–76.
[33] Kaempfen A, Todorov A, Guven S, Largo RD, Jaquiery C, Scherberich A, et al. Engraftment of prevascularized, tissue engineered constructs in a novel rabbit segmental bone defect model. Int J Mol Sci 2015;16(6):12616–30.
[34] Diomede F, Marconi GD, Fonticoli L, Pizzicanella J, Merciaro I, Bramanti P, et al. Functional relationship between osteogenesis and angiogenesis in tissue regeneration. Int J Mol Sci 2020;21(9).
[35] Fan H, Zeng X, Wang X, Zhu R, Pei G. Efficacy of prevascularization for segmental bone defect repair using beta-tricalcium phosphate scaffold in rhesus monkey. Biomaterials 2014;35(26):7407–15.
[36] Kawai T, Pan CC, Okuzu Y, Shimizu T, Stahl AM, Matsuda S, et al. Combining a vascular bundle and 3D printed scaffold with BMP-2 improves bone repair and angiogenesis. Tissue Eng 2021;27(23–24):1517–25.
[37] Liu X, Chen W, Zhang C, Thein-Han W, Hu K, Reynolds MA, et al. Co-seeding human endothelial cells with human-induced pluripotent stem cell-derived mesenchymal stem cells on calcium phosphate scaffold enhances osteogenesis and vascularization in rats. Tissue Eng 2017;23(11–12):546–55.
[38] Zhang W, Wray LS, Rnjak-Kovacina J, Xu L, Zou D, Wang S, et al. Vascularization of hollow channel-modified porous silk scaffolds with endothelial cells for tissue regeneration. Biomaterials 2015;56:68–77.
[39] Zhu S, Bennett S, Kuek V, Xiang C, Xu H, Rosen V, et al. Endothelial cells produce angiocrine factors to regulate bone and cartilage via versatile mechanisms. Theranostics 2020;10(13):5957–65.
[40] Cheng WX, Liu YZ, Meng XB, Zheng ZT, Li LL, Ke LQ, et al. PLGA/beta-TCP composite scaffold incorporating cucurbitacin B promotes bone regeneration by inducing angiogenesis. J Orthop Translat 2021;31:41–51.
[41] Shi GS, Li YY, Luo YP, Jin JF, Sun YX, Zheng LZ, et al. Bioactive PLGA/tricalcium phosphate scaffolds incorporating phytomolecule icaritin developed for calvarial defect repair in rat model. J Orthop Translat 2020;24:112–20.
[42] Maruyama M, Pan CC, Moeinzadeh S, Storaci HW, Guzman RA, Lui E, et al. Effect of porosity of a functionally-graded scaffold for the treatment of corticosteroid-associated osteonecrosis of the femoral head in rabbits. J Orthop Translat 2021;28:90–9.